ORIGINAL ARTICLE

The brain is hypothermic in patients with mitochondrial diseases

Mario Rango[1,2], Andrea Arighi[1,2], Cristiana Bonifati[1,2], Roberto Del Bo[1], Giacomo Comi[1] and Nereo Bresolin[1,2]

We sought to study brain temperature in patients with mitochondrial diseases in different functional states compared with healthy participants. Brain temperature and mitochondrial function were monitored in the visual cortex and the centrum semiovale at rest and during and after visual stimulation in seven individuals with mitochondrial diseases (n ¼ 5 with mitochondrial DNA mutations and n ¼ 2 with nuclear DNA mutations) and in 14 age- and sex-matched healthy control participants using a combined approach of visual stimulation, proton magnetic resonance spectroscopy (MRS), and phosphorus MRS. Brain temperature in control participants exhibited small changes during visual stimulation and a consistent increase, together with an increase in high-energy phosphate content, after visual stimulation. Brain temperature was persistently lower in individuals with mitochondrial diseases than in healthy participants at rest, during activation, and during recovery, without significant changes from one state to another and with a decrease in the high-energy phosphate content. The lowest brain temperature was observed in the patient with the most deranged mitochondrial function. In patients with mitochondrial diseases, the brain is hypothermic because of malfunctioning oxidative phosphorylation. Neuronal activity is reduced at rest, during physiologic brain stimulation, and after stimulation.

Keywords: activation; brain metabolism; brain temperature; mitochondrial diseases; recovery; visual stimulation

INTRODUCTION

Maintaining near-constant brain temperature (T_{br}) across a wide range of metabolic activity is critical for normal brain function.[1] However, brain temperature is an often-ignored parameter in neuroscience and clinical studies.

Animal studies have shown a close relationship between brain temperature and cerebral oxygen metabolic rate ($CMRO_2$)[2] at rest and during brain activation.[3] There are only fragmentary data regarding T_{br} and its regulation under different physiologic conditions and no temperature data are available regarding patients with mitochondrial disorders. Time-dependent variations in T_{br} are caused by fluctuations of cerebral blood flow (CBF) and $CMRO_2$, both of which appear to be coupled to changes in neuronal activity.[1] Increases in CBF reduce T_{br} and increases in brain metabolism increase T_{br}.[1]

Intense heat production is an essential feature of normal brain energetics; most of the energy used for brain functioning is eventually released as heat.[4] In the brain, heat is produced mostly by mitochondrial oxidative chemical reactions. Most of the energy required for brain activity is generated from the net chemical reaction of oxygen and glucose; some of this energy (33%) is immediately dissipated into heat, and the rest (67%) is used to synthesize ATP. The final ATP hydrolysis releases part of the energy back to the system as heat.[4]

Owing to rapid ATP turnover and the high cerebral metabolic rate of oxygen, basal heat production within the brain is high. Aerobic metabolism of glucose produces heat at a rate of 0.7 J/min per gram brain tissue.[4] In a closed system, this metabolism would lead to an increase in temperature of 0.28℃/min. However, because the brain is an 'open' thermodynamic system, heat is dissipated through circulation and by conduction through the skull. Most of the heat is dissipated through CBF, with venous blood leaving the brain at a higher temperature than the incoming arterial blood.[1,4]

Mitochondrial diseases are characterized by dysfunctions of mitochondria and energetics. In these diseases, cellular dysfunctions arise from disordered energy metabolism (i.e., failure of the respiratory chain to produce ATP). Primary (point mutations in mitochondrial DNA (mtDNA)) and secondary (e.g., due to polymerase gamma—POLG—mutations) mtDNA defects disrupt the formation of one or more mitochondrially encoded respiratory chain subunits, leading to respiratory chain dysfunction and compromised energy-generating capacity. As a consequence, the amount of heat released owing to brain metabolism is usually reduced.[5,6]

Some patients with mitochondrial disease appear to have problems regulating body temperature at higher or lower ambient temperatures, and exposure to cold can result in severe heat loss and trigger an energy crisis.[5,6]

Mitochondrial diseases are heterogeneous and often multisystemic. Because the mitochondrion provides much of the energy for the cell, mitochondrial disorders preferentially affect tissues with high-energy demands, such as the brain, although any organ can be affected.[5,6]

Thus, energetic defects have been implicated in forms of blindness, deafness, movement disorders, dementias, cardiomyopathy, myopathy, renal dysfunction, and aging.[5,6]

Mitochondrial diseases can be caused by genetic defects in any mtDNA or nuclear DNA (nDNA) gene that encodes a mitochondrial protein or structural RNAs. Given the energetics impairment, brain temperature is likely affected in mitochondrial diseases.

Most physical and chemical processes are affected by temperature, with the average van't Hoff coefficient Q10 ¼ 2.3[4] and temperature influences several biochemical and physiologic parameters involved in brain temperature control.[1] Indeed, in studies on brain slices, temperature increases enhanced oxygen metabolism.[7]

Neuronal activity is temperature dependent, with neuronal firing increasing with increased temperature.[1,8] Accordingly, decreasing temperature modifies neuronal activity in the visual cortex; in fact, studies of visual cortex neurons have shown that cooling (from 35°C to 21°C) decreases the membrane potential (1.0 to 2.0 mV/1°C) and increases the input resistance (B2MO/1°C), bringing the cells closer to the spiking threshold. Cooling also strongly increases the spike duration (from 1.3 ms at 32°C to 5.1 ms at 20°C).[9]

Studies of the visual cortex have also revealed various effects of temperature changes on passive membrane properties, single neuronal spikes, and spike bursts, as well as on the neuronal responses induced by direct and indirect electrical stimulation of tissue or its afferent pathways.[1,8–10]

Small temperature variations affect protein conformation and assembly and alter protein expression.[1,10] Temperature also strongly modulates neurotransmitter release.[1,11]

The brain is the most heat-sensitive organ in the human body,[1] and mitochondrial and plasma membranes are the most temperature-sensitive cellular elements, with hyperthermia potentiating the cytotoxic effects of reactive oxygen species.[1,10] Febrile temperature (40°C) activates mitochondrial energy-supplying functions; further temperature increase by only a few degrees leads to severe impairment of mitochondrial ability to maintain the membrane potential and synthesize ATP.

Less is known on how increased brain activity influences temperature. During functional stimulation, the major factors contributing to T_{br} regulation are changes in oxygen consumption, CBF, and the temperature of incoming arterial blood, as well as extensive heat exchange between the activated area and the surrounding brain tissue.[1] Cerebral blood flow , brain metabolism, and oxygen extraction all increase, that is, mechanisms that reduce heat work together with other mechanisms that increase local heat. As a consequence, the net heat balance, or T_{br}, is difficult to predict under these conditions because these changes do not occur simultaneously. Brain temperature measurement in animals and humans has yielded data that show either an increase or a decrease[12–15] in temperature during stimulation. Sensory stimulation results in T_{br} changes in either direction, partly depending on anatomic localization and these observations, altogether indicate that there may be variations, regarding both polarity and size, in the T_{br} due to brain activation. No consistent experimental data or mathematical modeling is available regarding T_{br} in the postactivation/recovery phase.

In control participants, mitochondrial function changes in a predictable manner during rest, brain stimulation/activation, and recovery from activation.[4,16] Instead, brain temperature changes under the same conditions are less well known in control participants and completely unknown in patients with mitochondrial diseases. Given their likely interdependence, we studied both

functional conditions (i.e., at rest, during functional activation, and after activation) in patients affected by mitochondrial citopathies and in control participants for comparison. We planned a study in which T_{br} was observed with a large temporal window, serially, across these different functional states in the visual cortex using a noninvasive visual stimulation-1-H magnetic resonance spectroscopy (1-H MRS) combined approach. We used 1-H MRS because it is the most reliable noninvasive brain thermometry method.[1] We observed mitochondrial function using 31-P MRS under the same conditions.[16]

PATIENTS AND METHODS

Patient Population

The study included five patients (two men, three women; mean age 46 years (s.d. 11)) with mitochondrial disease with mtDNA mutation without clinical central nervous system involvement (MDW/mtDNA) (Table 1). All participants had chronic progressive external ophthalmoplegia with or without limb myopathy. In all cases, the diagnosis of MDW/mtDNA was based on the clinical examination and the combined findings of histology, biochemical analysis, and genetic analysis of muscle biopsy specimens.[16] Southern blot analysis was performed on a muscle biopsy from each patient. Patients with single mtDNA deletion were selected (Table 1), and only patients with a quantified amount of mtDNA deletion between 40% and 60% were included in the study.

Full ophthalmologic and neurologic examinations, T1- and T2-weighted magnetic resonance imaging (MRI) brain studies and electroencephalography were performed to exclude patients with any of the following symptoms or signs of central nervous system involvement on neurologic examination, abnormal brain MRI studies, abnormal electroencephalogram, and abnormal ophthalmologic examinations (except for ptosis or impaired ocular motility). Patients with other diseases and patients taking drugs of any kind were also excluded.

Two patients with nuclear mitofusin 2 gene (MFN2) mutation with clinical peripheral and central nervous system involvement (MD/nDNA) were also included in the study (Table 1).[17] They were father and son, and both had mild cognitive impairment and peripheral neuropathy. The diagnosis of MD/nDNA was based on the clinical examination and the combined findings of histology, biochemical analysis, and genetic analysis of nerve biopsy specimens and blood.[16,17] All MFN2 gene exons were analyzed on leukocyte-derived DNA as described.[17] The coding exons of Berardinelli-Seip congenital lipodystrophy type 2 (BSCL2), vesicle-associated membrane protein associated protein B (VAPB), senataxin (SETX), glycyl-tRNA synthetase (GARS), and optic atrophy-1 (OPA1) genes were also sequenced.[17] The entire mtDNA sequence was analyzed from blood-derived DNA.

Fourteen control participants matched with MDW and MD patients for age (mean age 43 years, s.d. 11) and sex (8 men and 6 women) were studied. Each patient was matched with two control participants of the same age (age difference O5 years) and sex. Control participants were defined as having no history of neurologic disease, no history of major disease, normal neurologic and ophthalmologic examinations, and normal T1- and T2-weighted brain MRI; they were also not taking any drugs. The five oldest control participants also underwent pattern reversal visual-evoked potential, with normal results. Vascular risk factors were excluded.

Table 1. Patient information

Patient no.	Clinical phenotype	Age (years)	DNA mutation
1	CPEO	26	mtDNA common deletion
2	CPEO, limb myopathy	43	mtDNA common deletion
3	CPEO, limb myopathy	47	mtDNA common deletion
4	CPEO, limb myopathy	65	mtDNA single deletion (12,112–14,442)
5	CPEO	51	mtDNA single deletion (6,900–12,500)
6	Peripheral neuropathy, optic neuropathy, cognitive impairment	42	Nuclear DNA MFN2 heterozygous exon 4 nucleotide substitution (c.310C4T)
7	Peripheral neuropathy, cognitive impairment	10	Nuclear DNA MFN2 heterozygous exon 4 nucleotide substitution (c.310C4T)

CPEO, chronic progressive external ophthalmoplegia; mtDNA, mitochondrial DNA. For single deletion, the deleted region in mitochondrial DNA (nucleotides) is reported in parentheses.

In all subjects flash and pattern reversal visual-evoked potential were obtained. The study was approved by both the local and the national ethical committees. All study participants provided informed consent in accordance with the declaration of Helsinki.

This project has been approved by the National Institute of Health and by the local ethical committee. The procedures followed were in accordance with the Ethical Standards of the Fondazione Policlincico, IRCCS responsible committee on human experimentation (institutional) and with the Helsinki Declaration of 1975 (and as revised in 1983).

Visual Stimulation

The method used to deliver visual stimulation has been fully described.[16] In brief, it was delivered by goggles (Grass) that flashed at 8 Hz to reproduce the stimulation pattern used in a previous work.[16] The authors used an infrared-driven computerized system that was developed connected to the magnetic resonance (MR) system computer, through which goggles were automatically turned on after 6.5-minute acquisition and turned off after 13-minute acquisition.

Spectra were acquired at rest (first 6.5 minutes), during visual stimulation (next 6.5 minutes) and during recovery from visual activation (next 6.5 minutes).

Body Temperature Measurement

Axillary body temperature was measured with a mercury-in-glass thermometer in patients and in control participants. No febrile participant at the time of the study (body temperature $< 37^{\circ}C$) was included in the study. Participants sat in the waiting hall of the MRI unit for 60 minutes before their MRS assessment to ensure proper adaptation. The hall's temperature was maintained at $22^{\circ}C$ throughout all assessment periods. The magnet temperature was maintained at $22^{\circ}C$.

All studies were performed on the same day of the week between 1400 and 1600 h.

Brain Temperature Measurement using 1H Magnetic Resonance Spectroscopy

All studies were performed on a 1.5T Siemens System (Siemens, Erlangen, Germany) using a quadrature detection transmitter/receiver (Tx/Rx) head coil. The images were assessed under blinded conditions by an MR expert. Magnetic resonance sagittal, axial, and coronal T1 and T2/proton density weighted images were acquired.

Single-voxel 1H-MRS spectra were acquired without water suppression from a volume of interest (20_20_10 mm) aligned along the calcarine scissure of the occipital cortex and in the left centrum semiovale. A point-resolved spectroscopy sequence was used. The acquisition parameters were repetition time 2,000 ms, echo time 270 ms, 32 acquisitions, 1,024 points per spectrum, and 1,000 Hz spectral width.

Spectra were acquired at rest (baseline condition), during visual stimulation, and after the end of visual stimulation. Two spectra from the visual cortex were acquired (spectrum mid-acquisition time) 2 minutes after and 5 minutes after the beginning of each state. Similarly, two spectra were acquired from the centrum semiovale after the beginning of each state. The two temperature values obtained from the resting state were averaged to obtain a single value.

All spectra were inspected visually first, and discarded if they were judged to be of poor quality (e.g., had a badly elevated baseline or contained spurious peaks). Spectra were also discarded if linewidths at half maximum were < 8 Hz or if the metabolite peaks were offset from their expected values by > 0.1 p.p.m. Data processing included Lorentzian filtering (1 Hz line broadening), Fourier transformation, and automatic phase correction.

A typical spectrum obtained from the visual cortex is displayed in Figure 1. The temperature calculation was based on the measured difference between the water resonance frequency, which is linearly temperature dependent, and the N-acetyl aspartate (NAA) methyl resonance frequency, which remains stable at different temperatures.[18,19]

Absolute values of T_{br} (expressed in $^{\circ}C$) were calculated according to the equation $T1 = 228.2 - 72.2\_(d_{H2O} - d_{NAA})$,[19] where d_{H2O} and d_{NAA} are the resonance frequencies expressed in p.p.m., measured at the center of the water-fitted and NAA-fitted peaks. We employed a time domain analysis using the jMRUI software (URL http://www.mrui.uab.es/mrui/). The water and NAA signal were modeled as mono-exponentially decaying sinusoids using the Hankel Lanczos Total Least Squares (HLTLS) algorithm[20] and their resonance frequency estimated. The digital sensitivity
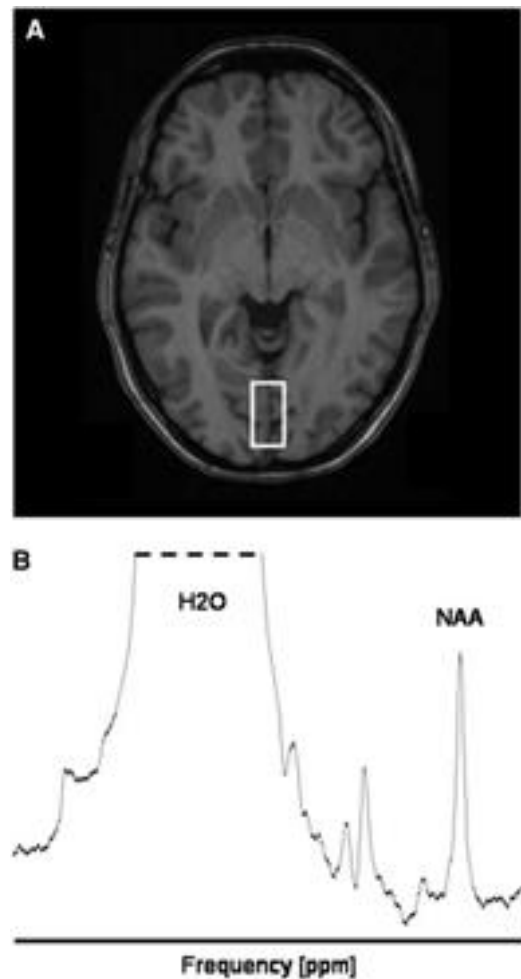

Figure 1. Visual cortex spectrum and brain temperature. 1H magnetic resonance (MR) unfitted spectrum (B) obtained from a voxel of 20_20_10 mm centered on the calcarine scissure of a healthy volunteer (A). Spectra acquisition parameters: point-resolved spectroscopy sequence (PRESS), repetition time (TR) 2,000 ms, echo time (TE) 270 ms. The MR signals corresponding to water (H_2O) and N-acetyl-aspartate (NAA) are identified. Brain temperature is obtained by measuring the resonance frequency of H_2O and NAA, according to the formula $T1 = 228.2 - 72.2\_(d_{H2O} - d_{NAA})$, where $T1$ is temperature in degree Celsius and d_{H2O} and d_{NAA} are the resonance frequencies expressed in p.p.m., measured at the center of the water-fitted and NAA-fitted peaks. The digital sensitivity of this MR thermometry method is 0.0103 p.p.m./$1^{\circ}C$. The actual measured sensitivity is within $0.20^{\circ}C$ (see Supplementary File 1). The actual measured accuracy is within $0.20^{\circ}C$ (see Supplementary File 1) as well. For these reasons, we rounded brain temperature values at $0.20^{\circ}C$ steps.

of this MR thermometry method is 0.0103 p.p.m./$1^{\circ}C$. The actual measured sensitivity is within $0.20^{\circ}C$ (see Supplementary File 1). The actual measured accuracy is within $0.20^{\circ}C$ (see Supplementary File 1) as well. For these reasons, we rounded brain temperature values at $0.20^{\circ}C$ steps.

31-P Magnetic Resonance Spectroscopy Spectra

Spectra were obtained from the visual cortex and analyzed as described previously.[16] The phosphocreatine þ bATP variable, a measure of mitochondrial function,[16] was calculated by peak integration and then used for the following calculations. The values were normalized to the reference compound signal and expressed in arbitrary units.[16] For the purpose of the study, the stimulation 1 and stimulation 2 periods were lumped together, as were the recovery 1 and recovery 2 periods.

Visual-Evoked Potential

Both flash and pattern visual-evoked potentials were recorded. Pattern visual-evoked potentials were recorded mono-ocularly to reversal of fulfilled checkerboards. Check size was 50'. The mean luminescence was 50 cd/m^2 with a contrast of 90%, 128 sweeps were averaged per recording. All subjects wore their best refractory correction. The stimulated eye fixed a reference point at the center of the monitor, while the other eye was blinded by a pad. This setting guaranteed an approximately similar luminescence on each eye. The evaluated variable, for the purpose of this study, was the P100 latency.

Statistics

Two-tailed t-tests, analysis of variance, and Pearson's r correlation coefficients were used for statistical analysis. Bonferroni's correction for multiple comparisons was applied. All P-values lower than 0.001 were rounded at 0.001 and reported as P⊙0.001.

RESULTS

Body Temperature

The mean body temperature did not differ between patients with mitochondrial disease and control participants (36.70IC, 0.13 s.d. vs. 36.60IC, 0.11 s.d., P ¼ n.s.).

Control Participants

At rest, the mean T_{br} in the visual cortex was 37.40IC (s.d. 0.20). At 2 minutes after the beginning of visual stimulation, the mean T_{br} was still 37.40IC (s.d. 0.20) (P ¼ n.s.) (Figure 2). At 5 minutes, the mean T_{br} decreased to 37.20IC (s.d. 0.20) (0.20IC below the baseline value, P⊙0.05) (Figure 2). The mean T_{br} at 2 minutes after the end of visual stimulation rose significantly to 37.80IC (s.d. 0.20) (0.40IC above baseline value, P⊙0.0001) (Figure 2). At 5 minutes after the end of visual stimulation, the mean T_{br} returned to 37.40IC (s.d. 0.20), thus overlapping the baseline value (P ¼ n.s.; Figure 2).

Analysis of variance did not reveal any mean temperature changes in the centrum semiovale across the five states (rest, activation 1, activation 2, recovery 1, and recovery 2) (P ¼ n.s.). At rest, the mean T_{br} was 37.60IC (s.d. 0.20). The mean T_{br} was 37.60IC (s.d. 0.20, P ¼ n.s.) at 2 minutes after initiating visual stimulation, and 37.60IC (s.d. 0.26, P ¼ n.s.) at 5 minutes after initiating visual stimulation. At 2 minutes after the end of visual

stimulation, the mean T_{br} was 37.60IC (s.d. 0.20, P ¼ n.s.); at 5 minutes after the end of visual stimulation, the mean T_{br} was 37.60IC (s.d. 0.20, P ¼ n.s.). Flash and pattern reversal visual-evoked potentials were normal in all subjects.

MDW/Mitochondrial DNA Patients

At rest, the T_{br} in the visual cortex was below the normal range (37.00IC to 37.80IC) in all the five patients.

Analysis of variance revealed that the mean T_{br} in the visual cortex was significantly lower in patients with mtDNA mutations than in control participants. This was true for all five functional states (rest, visual stimulation 1, visual stimulation 2, recovery 1, and recovery 2) (P⊙0.001; Figure 2). T_{br} (in IC) was at rest, 36.60 (0.20) vs. 37.40 (0.20) (P⊙0.001); during the first part of visual stimulation, 36.60 (0.40) vs. 37.40 (0.20) (P⊙0.001); during the second part of visual stimulation, 36.60 (0.40) vs. 37.20 (0.20) (P⊙0.001); during the first part of recovery, 36.60 (0.40) vs. 37.80 (0.20) (P⊙0.001); and during the second part of recovery, 36.60 (0.20) vs. 37.40 (0.20) (P⊙0.001).

In the centrum semiovale, the T_{br} at rest was below the normal range (37.20IC to 38.20IC) in all five patients and the mean T_{br} at rest was lower in patients with mtDNA mutations than in control participants: 36.80IC (0.40) vs. 37.60IC (0.20), P⊙0.001, unpaired t-test.

MD/Nuclear DNA Patients

In the visual cortex, the T_{br} at rest was below the normal range in the two MDW/mtDNA patients (35.80 and 36.40, respectively). In the centrum semiovale, the T_{br} at rest was also below the normal range in the two MDW/mtDNA patients (35.80IC and 36.60IC, respectively).

At rest, the PCr þ bATP was normal in all mitochondrial patients except for patient 6, who had an abnormally low value (Figure 3). For this reason and because he had optic neuropathy, the 31-P MRS study was performed only at rest in this patient. PCr þ bATP remained in the normal range during visual stimulation in the other six patients, but decreased below normal during recovery in all participants (Figure 3). Spectra from a normal subject and from a patient during recovery are shown in Figure 4.

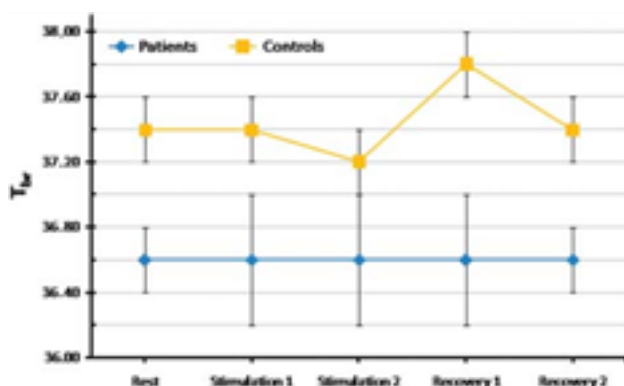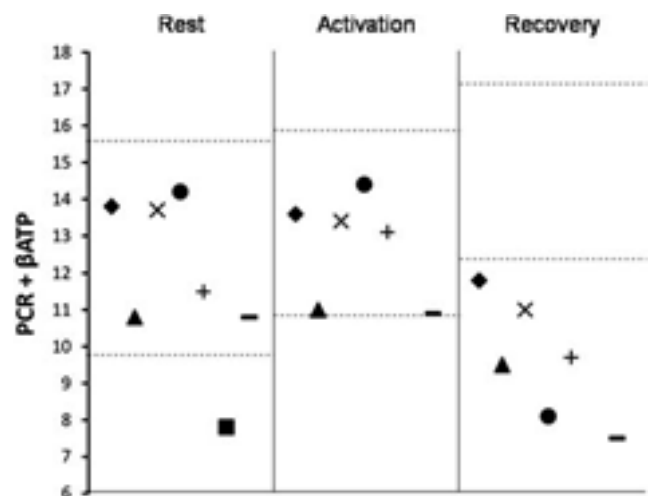Figure 2. The mean temperature (±s.d.) of the visual cortex in MDW/mtDNA patients and in healthy control participants at rest, during visual stimulation, and during recovery after visual stimulation. T_{br} remains flat and constantly lower in the MDW/mtDNA group than in the healthy control participants. In the control group, after a small decrease in the second part of stimulation, T_{br} increases during the first part of recovery. Stimulation 1, first part of visual stimulation; Stimulation 2, second part of visual stimulation; Recovery 1, first part of recovery from visual stimulation; Recovery 2, second part of recovery from visual stimulation.

Figure 3. Single phosphocreatine (PCr) þ bATP values of patients at rest, during visual stimulation, and during recovery. Patient 1, solid diamond; Patient 2, solid triangle; Patient 3, x; Patient 4, solid circle; Patient 5, þ; Patient 6, solid square; Patient 7, black bar. For the purpose of the study, the two stimulation and two recovery periods have each been pooled. The normal range for each condition is bounded by the dotted lines.

Flash visual-evoked potential was normal in all patients except in patient #6. Pattern reversal visual-evoked potentials showed increased mean P100 latency in the pooled MDW/mtDNA and MD/nDNA patient group (128 ± 14 ms vs. 87 ± 15 ms, P○0.01). A negative correlation (P○0.01) between visual cortex rest T_{br} and P100 latency was found by a Pearson's r correlation coefficient analysis including all seven patients.

DISCUSSION

This is the first study observing sequential brain temperature variations across functional states in control participants and in patients with mitochondrial disorders. We used a large temporal window because the time constant of the temperature change is several seconds.[13]

In control participants, T_{br} at rest was higher than body temperature in line with previous measurement.[1] The T_{br} of the stimulated region in control participants first remained stable and then decreased slightly. These findings help to explain contradictory results of short stimulation studies[21] vs. longer stimulation studies.[22] Although other kinds of stimuli may be used, we chose to study the visual cortex because visual activation of the brain appears optimal given the high oxidative metabolism[4,11] and high levels of oxidative phosphorylation enzymes in the visual cortex.[23] Additionally, visual stimuli can be easily graded.[24]

Glycolysis, which releases less heat per mole of glucose than respiration, appears to prevail during the first part of brain activation, while respiration prevails during the second part.[25] Although CBF increases significantly during functional activation and brain metabolism also increases, the exact timing of these changes and their relationship are unclear.

In control participants during activation, our data can be explained by a change in the ratio of CBF to glucose metabolism (CBF/CMRglu), by a change in the ratio of CBF to oxygen metabolism (CBF/CMRO), or by a change in both within the time interval that we observed.[25] Cerebral blood flow returns to baseline almost immediately after the end of brain activation,[26]
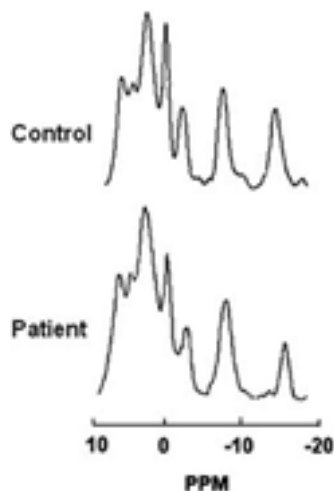

Figure 4. 31-P spectra from a control subject and from a patient during recovery from visual activation. Spectra acquisition/processing parameters: sweep width ¼ 2,000 Hz, 2,048 digitalized points, convolution difference to remove broad signal (exponential line broadening ¼ 150 Hz), exponential multiplication (20 Hz) to improve signal-to-noise ratio, and no baseline correction. Please, note that both phosphocreatine (0 p.p.m.) and bATP (ÿ 19 p.p.m.) peaks are lower in the patient than in the control subject (whereas they started from similar values at rest, not shown here).

while oxygen metabolism and glucose metabolism remain elevated.[27] As a result, an excess of heat is released from the brain that is not adequately removed by increased CBF. This situation causes the T_{br} to increase during the first part of the postactivation phase, with a return toward baseline values during the second part when oxygen metabolism decreases.[26] This is the first report to show that in humans T_{br} increases after activation is over (i.e., after the end of increased neuronal firing).

This finding has several physiologic implications. First, during neuronal firing there is little heat release. Second, there is an aftermath of increased brain activity that extends for several minutes beyond the activation phase itself; this aftermath is dynamic, with a progressive return to baseline conditions. This information must be taken into account if a new stimulus is delivered to the brain before a proper postactivation/recovery interval is observed: in this case, the starting conditions differ from when a proper postactivation interval is observed.

Lack of a proper postactivation interval happens in everyday life; for example, driving a car at night on the highway or dancing with stroboscopic lights implies a great amount of closely repeated visual stimulation that is not present when resting in bed with the lights off.[28] It is also the case for most experimental studies with averaged prolonged stimulation blocks, since they usually observe too short (subminute) interstimulation intervals.[29] This is especially important in blood oxygen level-dependent magnetic resonance studies, as oxygen release from hemoglobin is temperature dependent and a change in blood oxygen level-dependent signal may actually reflect temperature changes.[29,30]

The change of 0.60◦C that we observed in the visual cortex between the second part of visual stimulation and the first part of recovery represents, physiologically, a very consistent temperature change in a short time, which may strongly influence brain function since the increase in brain temperature increases neuronal firing.[1,8] There may be also consequences to CBF of changes in brain temperature. In fact, there is some evidence that selective brain cooling increases CBF above control levels and vice versa.[31]

In patients with mitochondrial diseases T_{br} at rest is decreased. Indeed, except for a single instance of ATP synthase deficiency, mitochondrial diseases are characterized by reduced brain CMRO at rest with reduced heat release.[32,33] This way, body temperature and brain temperature overlap because brain temperature cannot be kept elevated by the consistent production of heat by the brain, as in control participants. Indeed, in our study the lowest T_{br} was observed in the patient (#6) with the most deranged respiratory chain (i.e., the patient whose brain high-energy phosphates were already reduced at rest).

In turn, low T may have several effects. First, it has a protective effect on mitochondria.[34] It tends to increase local blood flow, and reduces the temperature-dependent release of oxygen from hemoglobin. Hypothermia reduces cerebral glucose and oxygen metabolism, but maintains a slightly better energy level, which indicates that ATP breakdown is reduced more than ATP synthesis.[35]

Neurons are among the most metabolically active cells, and most of the ATP generated is used for impulse generation and transmission. An estimated 40% to 50% of the energy goes to maintain membrane potential by driving the membrane sodium–potassium ATPase pump,[4] while the remaining energy is consumed for synaptic transmission, calcium homeostasis, and other cellular processes including axonal transport. Because neuronal activity, CMRO , ATP content, and T are tightly linked,[4,11] the findings of low ATP content and low T in light of previous reports of reduced $CMRO_2$[32–34] suggest that neuronal activity is reduced at rest in patients with mitochondrial diseases. This finding might help to explain the brain dysfunction and symptoms observed in patients with lower T_{br}.

The T_{br} curve of mitochondrial patients remains substantially flat during and after brain activation, with all values lower than the

T_{br} in the corresponding functional states in control participants. Because physiologically T_{br} is mainly affected by $CMRO_2$ during functional challenges, this finding suggests that the defective respiratory chain, beyond underfunctioning at rest, cannot increase $CMRO_2$ any further in response to increased demands,[36] which also seems to be confirmed in our study by decreased high-energy phosphate content during the post-activation phase. In the normal brain, high-energy phosphates (which contain energy used for brain functioning) are mostly synthesized through oxidative pathways, with the ratio of oxygen use to glucose use maximally increased during the postactivation phase compared with activation and rest.[37,38] These findings also suggest that neurons most likely do not activate appropriately during brain stimulation in individuals with mitochondrial diseases as suggested by the finding of abnormal pattern reversal visual-evoked potentials in these patients. These considerations may have important implications when studying brain activation and brain functions in patients with mitochondrial dysfunction.[36]

DISCLOSURE/CONFLICT OF INTEREST

The authors declare no conflict of interest.

REFERENCES

1 Rango M, Arighi A, Bresolin N. Brain temperature: what do we know? Neuroreport 2012; 23: 483–487.
2 Michenfelder JD, Milde JH. The relationship among canine brain temperature, metabolism, and function during hypothermia. Anesthesiology 1991; 75: 130–136.
3 Trübel HK, Sacolick LI, Hyder F. Regional temperature changes in the brain during somatosensory stimulation. J Cereb Blood Flow Metab 2006; 26: 68–78.
4 Siesjo B. Brain energy metabolism. Wiley: New York, 1978.
5 Chaturvedi RK, Flint Beal M. Mitochondrial diseases of the brain. Free Radic Biol Med 2013; 63: 1–29.
6 Schapira AH. Mitochondrial diseases. Lancet 2012; 379: 1825–1834.
7 Nishizaki T, Yamauchi R, Tanimoto M, Okada Y. Effects of temperature on the oxygen consumption in thin slices from different brain regions. Neurosci Lett 1988; 86: 301–305.
8 Tang B, Kalatsky VA. Influence of body temperature on the evoked activity in mouse visual cortex. Brain Imaging Behav 2012; 7: 177–187.
9 Volgushev M, Vidyasagar TR, Chistiakova M, Yousef T, Eysel UT. Membrane properties and spike generation in rat visual cortical cells during reversible cooling. J Physiol 2000; 522 Pt 1: 59–76 Erratum in: J Physiol 2000;528(Pt 3):669.
10 Kiyatkin EA. Brain temperature homeostasis: physiological fluctuations and pathological shifts. Front Biosci 2010; 15: 73–92.
11 Siegel GJ, Albers RW, Agranoff BW, Katzman R. Basic neurochemistry. Little Brown: Boston, MA, 1981.
12 Trubel HK, Sacolick LI, Hyder F. Regional temperature changes in the brain during somatosensory stimulation. J Cereb Blood Flow Metab 2006; 26: 68–78.
13 Kiyatkin EA, Brown PL, Wise RA. Brain temperature fluctuation: a reflection of functional neural activation. Eur J Neurosci 2002; 16: 164–168.
14 George JS, Lewine JD, Goggin AS, Dyer RB, Flynn ER. IR thermal imaging of a monkey's head: local temperature changes in response to somatosensory stimulation. Adv Exp Med Biol 1993; 333: 125–136.
15 Gorbach AM, Heiss J, Kufta C, Sato S, Fedio P, Kammerer WA et al. Intraoperative infrared functional imaging of human brain. Ann Neurol 2003; 54: 297–309.
16 Rango M, Bozzali M, Prelle A, Scarlato G, Bresolin N. Brain activation in normal subjects and in patients affected by mitochondrial disease without clinical central nervous system involvement: a phosphorus magnetic resonance spectroscopy study. J Cereb Blood Flow Metab 2001; 21: 85–91.
17 Del Bo R, Moggio M, Rango M, Bonato S, D'Angelo MG, Ghezzi S et al. Mutated mitofusin 2 presents with intrafamilial variability and brain mitochondrial dysfunction. Neurology 2008; 71: 1959–1966.
18 Cady EB, D'Souza PC, Penrice J, Lorek A. The estimation of local brain temperature by in vivo 1H magnetic resonance spectroscopy. Magn Reson Med 1995; 33: 862–867.
19 Corbett R, Laptook A, Weatherall P. Noninvasive measurements of human brain temperature using volume-localized proton magnetic resonance spectroscopy. J Cereb Blood Flow Metab 1997; 17: 363–369.
20 Zhu M, Bashir A, Ackerman JJ, Yablonskiy DA. Improved calibration technique for in vivo proton MRS thermometry for brain temperature measurement. Magn Reson Med 2008; 60: 536–541.
21 Katz-Brull R, Alsop DC, Marquis RP, Lenkinski RE. Limits on activation induced temperature and metabolic changes in the human primary visual cortex. Magn Reson Med 2006; 56: 348–355.
22 Yablonskiy DA, Ackerman JJ, Raichle ME. Coupling between changes in human brain temperature and oxidative metabolism during prolonged visual stimulation. Proc Natl Acad Sci USA 2000; 97: 7603–7608Erratum in: Proc Natl Acad Sci USA 2000; 97:9819.
23 Martin JH. Neuroanatomy. Appleton & Lange: Stanford, CA, 1996.
24 Marrett S, Fujita H, Kuwabara H, Yasuhara Y, Ribiero L, Meyer E et al. Stimulus specific increase of oxidative metabolism in visual cortex. Society for Neuroscience Abstracts 1992; 18: 1394.
25 Frahm J, Krüger G, Merboldt KD, Kleinschmidt A. Dynamic uncoupling and recoupling of perfusion and oxidative metabolism during focal brain activation in man. Magn Reson Med 1996; 35: 143–148.
26 Lu Hanzhang, Golay Xavier, Pekar James J, van Zijl Peter CM. Sustained post-stimulus elevation in cerebral oxygen utilization after vascular recovery. J Cereb Blood Flow Metab 2004; 24: 764–770.
27 Madsen PL, Linde R, Hasselbach S, Paulson O, Lassen N. Activation-induced resetting of cerebral oxygen and glucose uptake in the rat. J Cereb Blood Flow Metab 1998; 18: 742–748.
28 Kandel ER, Schwartz JH, Jessel TM. Principles of neural science. Elsevier: New York, NY, 1991.
29 Kim SG, Ogawa S. Biophysical and physiological origins of blood oxygenation level-dependent fMRI signals. J Cereb Blood Flow Metab 2012; 32: 1188–1206.
30 Siggaard-Andersen O, Wimberley PD, Göthgen I, Siggaard-Andersen M. A mathematical model of the hemoglobin-oxygen dissociation curve of human blood and of the oxygen partial pressure as a function of temperature. Clin Chem 1984; 30: 1646–1651.
31 Kuluz JW, Prado R, Chang J, Ginsberg MD, Schleien CL, Busto R. Selective brain cooling increases cortical cerebral blood flow in rats. Am J Physiol 1993; 265(3 Pt 2): H824–H827.
32 Shishido F, Uemura K, Inugami A, Tomura N, Higano S, Fujita H et al. Cerebral oxygen and glucose metabolism and blood flow in mitochondrial encephalomyopathy: a PET study. Neuroradiology 1996; 38: 102–107.
33 Kondo S, Tanaka M, Osawa T, Okamoto K, Hirai S. Cerebral circulation and metabolism in patients with mitochondrial myopathies. Rinsho Shinkeigaku 1993; 33: 1033–1038.
34 Nemoto EM, Klementavicius R, Melick JA, Yonas H. Suppression of cerebral metabolic rate for oxygen (CMRO2) by mild hypothermia compared with thiopental. J Neurosurg Anesthesiol 1996; 8: 52–59.
35 Erecinska M, Thoresen M, Silver IA. Effects of hypothermia on energy metabolism in Mammalian central nervous system. J Cereb Blood Flow Metab 2003; 23: 513–530Review.
36 Vafaee MS, Meyer E, Gjedde A. Impaired activation of oxygen consumption and blood flow in visual cortex of patients with mitochondrial encephalomyopathy. Ann Neurol 2000; 48: 676–679.
37 Van Zijl P, Hanzhang J. The BOLD post-stimulus undershoot, one of the most debated issues in fMRI. NeuroImage 2012; 62: 1092–1102.
38 Madsen PL, Cruz NF, Sokoloff L, Dienel GA. Cerebral oxygen/glucose ratio is low during sensory stimulation and rises above normal during recovery: excess glucose consumption during stimulation is not accounted for by lactate efflux from or accumulation in brain tissue. J Cereb Blood Flow Metab 1999; 19: 393–400.